Convective Diffusional Analysis for Drug Transport through a Tubular Polymeric Membrane

D. R. FLANAGAN *x **and S. H. YALKOWSKY** ‡

Abstract □ The transport of three *p*-aminobenzoate esters (ethyl, butyl, and hexyl) through a tubular dimethyl polysiloxane membrane into a flowing liquid was investigated. The tubular configuration permits the exact determination of the convective diffusional contribution to membrane transport with models that account for fluid hydrodynamics. The observed transport behavior ranged from complete convective diffusion control for the hexyl ester to complete membrane control for the ethyl ester; the butyl ester exhibited a change in control with flow rate. The implications of convective diffusional considerations to intestinal absorption and dissolution studies are discussed.

Keyphrases □ Diffusion—three *p*-aminobenzoate esters through tubular dimethyl polysiloxane membrane into a flowing liquid □ Transport, drug—three *p*-aminobenzoate esters through tubular dimethyl polysiloxane membrane into a flowing liquid □ Membrane permeation—three *p*-aminobenzoate esters through tubular dimethyl polysiloxane membrane into a flowing liquid

Most studies on the transport of drugs through model membranes (1–3) have utilized transport systems with reproducible hydrodynamics and maximal surface-to-volume ratios. The stagnant diffusion layer or film model has been applied as a convenient tool for the interpretation of diffusional resistances in or on either side of the model membranes. The convenience and wide application of this model have led to the implication that it accurately reflects physical reality (4), but its limitations have been known for some time, particularly its weakness in predicting convective influences on mass transfer without use of empirical relationships (5).

By changing the experimental design for membrane transport studies, it will be shown that the convective diffusional contributions to mass transfer can be exactly determined with models that are more accurate pictures of physical reality. The experimental design utilizes a tubular membrane with an aqueous solution flowing at a constant rate through the tube. Such a system can be assembled easily and inexpensively to provide the advantages of previous systems plus the added advantage of being able to determine exactly the aqueous convective diffusional contribution to the overall transport rate. These studies also have important implications for intestinal absorption and dissolution studies.

THEORY

For an experimental design in which a flowing liquid is taking up solute from a tube wall, several models predict the extent of solute uptake under various convective conditions. The first type of convective condition may be termed plug flow (Fig. 1*a*), in which there is no velocity gradient in the flowing liquid. In this model, all liquid in the tube moves at a constant velocity, V_0, and the solute is taken up from the wall as the liquid flows through the tube. For a tube of a particular length, L, a constant solute concentration, C_{av}, is expected to be flowing out of the end if the flow rate is held constant. The differential equation describing the mass transfer due to convection and diffusion for this situation is:

$$V_0 \frac{\partial c}{\partial z} = D \frac{1}{r} \frac{\partial}{\partial r}\left(r \frac{\partial c}{\partial r}\right) \qquad \text{(Eq. 1)}$$

where $\partial c/\partial z$ = longitudinal concentration gradient, D = diffusion coefficient, r = radius, and $\partial c/\partial r$ = radial concentration gradient.

Equation 1 equates the convective contribution, $V_0(\partial c/\partial z)$, to the diffusional contribution:

$$D \frac{1}{r} \frac{\partial}{\partial r}\left(r \frac{\partial c}{\partial r}\right)$$

at steady state. This differential equation can be solved for the boundary conditions $C = 0$ at $z = 0$ for all r and $C = C_s$ (solute solubility in liquid at $r = R$, the inner radius of tube for all z) to give:

$$C_{av}/C_s = 1 - 4 \sum_{n=1}^{\infty} \frac{1}{\alpha_n} \exp\left(\frac{-\alpha_n DL}{V_0 R^2}\right) \qquad \text{(Eq. 2)}$$

where the α_n's are roots for the Bessel function, $J_0(r) = 0$. Equation 2 is an exact expression for C_{av} in terms of measurable quantities (C_s, D, L, V_0, and R) for systems adhering to the previously mentioned flow and boundary conditions.

A second, more physically realistic model is one in which the liquid velocity profile is not flat but parabolic (Fig. 1*b*). A parabolic velocity profile is in accordance with the prediction of the Navier–Stokes equations for laminar fluid flow in a tube (6). For this parabolic model, the fluid velocity is not a constant, V_0, but varies parabolically across the tube and can be characterized by a maximum velocity, V_{max}, or an average velocity, V_{av}. The differential equation describing mass transfer with a parabolic velocity profile is:

$$V_{max}\left[1 - \left(\frac{r}{R}\right)^2\right] \frac{\partial c}{\partial z} = D \frac{1}{r} \frac{\partial}{\partial r}\left(r \frac{\partial c}{\partial r}\right) \qquad \text{(Eq. 3)}$$

Equation 3 is identical to Eq. 1 for the diffusive contribution while differing in the convective term, which defines the flow conditions. A solution to Eq. 3 can be obtained numerically (7) with the same boundary conditions for Eq. 1 and takes the form:

$$C_{av}/C_0 = 1 - \sum_{n=1}^{\infty} a_n \exp\left(-\frac{b_n DL}{V_{av} R^2}\right) \qquad \text{(Eq. 4)}$$

where a_n and b_n are constants that have been determined numerically up to $n = 11$ (7). As in the plug flow model (Eq. 2), Eq. 4 for parabolic flow is an exact expression for C_{av} in terms of measurable quantities.

A third model involves parabolic flow with the added constraint that the solute concentration gradient does not penetrate to a great distance into the flowing fluid (8). Therefore, the diffusing solute is subjected to a velocity gradient that is essentially linear. With this assumption, the convective term in the differential equation for mass transfer becomes $V_{max}[2(R - r)/R]$, with $r \simeq R$ rather than the convective term given on the left-hand side of Eq. 3. The mass transfer differential equation thus becomes:

$$V_{max} 2 \frac{(R - r)}{R} \frac{\partial c}{\partial z} = D \frac{1}{r} \frac{\partial}{\partial r}\left(r \frac{\partial c}{\partial r}\right) \qquad \text{(Eq. 5)}$$

Again, the diffusive expression in Eq. 5 is identical to that in the previous models, with the difference being the convective expression. The solution to Eq. 5 becomes:

$$C_{av}/C_s = 2.53 \left(\frac{DL}{V_{av} R^2}\right)^{2/3} \qquad \text{(Eq. 6)}$$

This third model can be considered an asymptotic solution of the parabolic model, which is applicable when $DL/V_{av}R^2$ is small. Since Eq. 6 does not involve a power series or the need to evaluate constants (a_n and b_n) numerically, it is easier to handle mathematically than Eq. 4 within its limits of applicability. All of these models are similar in explicitly accounting for the increase in solute concentration as fluid travels down the tube, which continuously reduces the concentration gradient and diffusional flux, and differ only in their treatment of the convective contribution.

An inspection of Eqs. 2, 4, and 6 shows that the dimensionless term $DL/V_{av}R^2$ (for plug flow $V_0 = V_{av}$) is common to each and can be considered as a single variable, Z. Figure 2 shows a log–log plot of C_{av}/C_s predicted by the three models *versus* the variable Z. Graphically, it can be seen that the parabolic model (Eq. 4) and its asymptotic solution (Eq. 6) approach each other as Z decreases. The plug flow model (Eq. 2) gives

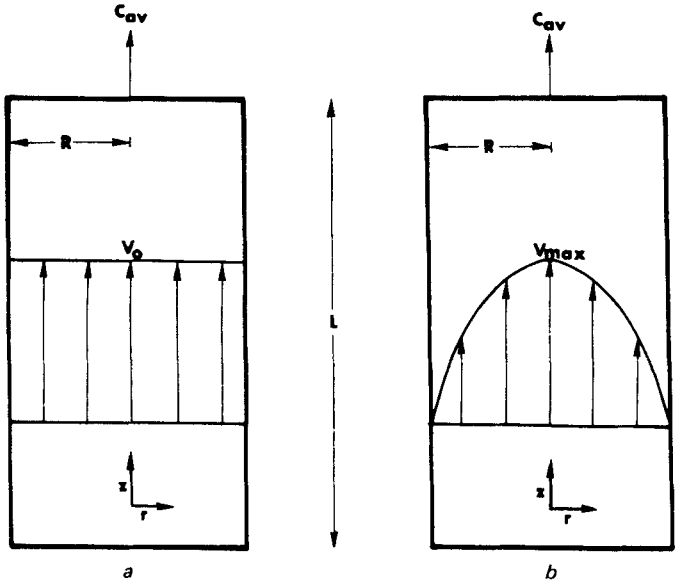

Figure 1—*Velocity profiles for liquid flow in a tube. Key:* a, *plug flow; and* b, *parabolic flow.*

the highest prediction of C_{av}/C_s throughout, with a limiting slope of 0.5 at low Z.

To evaluate the applicability of these models to experimental data, one must obtain steady-state values of C_{av} (effux concentration from the tube) for constant liquid flow rates in a tube of known diameter and length. By using the diffusion coefficient, D, and the solubility, C_s, of the solute in the liquid, the appropriate Z value and the ratio C_{av}/C_s can be calculated for each flow rate. The agreement of these model predictions can then be graphically compared with experimental data. Such comparisons of these models with experiment were conducted for solid tubes dissolving into flowing aqueous media (9).

For the application of convective diffusion models to membrane systems, an expansion of these equations is required to include a contribution due to membrane permeability. Under limiting conditions where membrane permeability is much higher than the mass transfer rate through the flowing fluid, the previously derived models can be applied without modification. Such limiting conditions imply that experimental studies on systems adhering exactly to Eq. 2, 4, or 6 would characterize only the convective diffusional properties of the solute in the flowing liquid and not the permeability of the membrane. At the opposite extreme, limiting conditions can be approached at which the membrane transport resistance is much higher than the convective diffusional resistance of the solute in the flowing liquid. At this limit, the effluent concentration, C_{av}, decreases linearly with flow rate. Between these limits, the transport behavior of a tubular membrane system exhibits varying contributions of membrane and convective diffusion control.

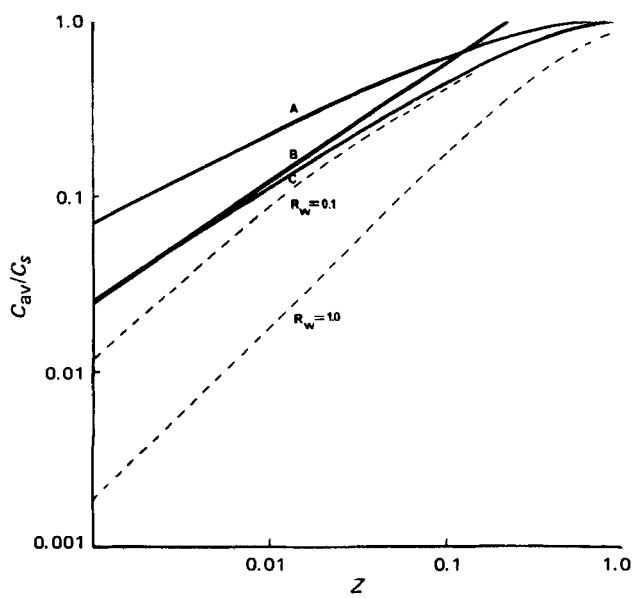

Figure 2—*Log–log plot of* C_{av}/C_s *versus* Z *for plug flow (A), parabolic asymptote (B), parabolic flow (C), and parabolic flow with wall resistance (- - -).*

Table I—Physical Constants for *p*-Aminobenzoate Esters

Compound	Membrane–Water Partition Coefficient[a]	Aqueous Diffusion Coefficient[b], $cm^2/sec \times 10^6$	Membrane Diffusion Coefficient[a], $cm^2/sec \times 10^6$
Ethyl ester	0.33	6.4	2.7
Butyl ester	3.90	6.0	2.7
Hexyl ester	46.90	5.7	2.7

[a] From Ref. 3. [b] Calculated from equations given in Ref. 15.

This behavior, of course, is not unique to tubular membrane systems. However, in this case the convective diffusional contribution in the flowing liquid is explicit and can be determined exactly without resort to semiempirical methods. The transport characteristics of liquids flowing with a parabolic velocity gradient in tubular systems with a contribution from wall resistance were treated analytically for heat transfer (10) and extended to mass transfer systems (11, 12). The treatment for mass transfer utilizes a wall resistance term, R_w, given by:

$$R_w = \frac{D_{aq}}{D_m P} \ln\left(\frac{\text{o.d.}}{\text{i.d.}}\right) \qquad \text{(Eq. 7)}$$

where D_m = membrane diffusion coefficient, D_{aq} = aqueous (liquid) diffusion coefficient, P = partition coefficient (membrane/aqueous), o.d. = outer tube diameter, and i.d. = inner tube diameter.

Figure 2 (dashed curves) shows the deviations from the parabolic model for selected values of R_w. As R_w increases, the effluent concentration, C_{av}, decreases at a particular Z value; as Z varies, the influence of a particular value of R_w on C_{av} also varies. At low Z, a particular R_w causes larger deviations from convective diffusion control than at high Z where the contribution can be small or negligible.

EXPERIMENTAL

Materials—The ethyl (benzocaine), butyl (butamben), and hexyl esters of *p*-aminobenzoic acid were obtained commercially[1] (ethyl and butyl) or synthesized (hexyl) (3). Table I includes the physical constants for these esters required for evaluating the transport data according to the theoretical equations. Medical grade silicone tubing[2] (dimethyl polysiloxane) was used in 1-m lengths with an inside diameter of 1.47 mm and an outside diameter of 1.96 mm. Deionized water was used throughout.

Analytical Procedures—All analyses for *p*-aminobenzoate esters were conducted spectrophotometrically[3] at 285 nm.

Membrane Transport Systems—The two experimental transport configurations differed from each other only by the degree of curvature of the tubing. The tubing was either threaded through stainless steel paper clips soldered to a circular stainless steel rod and mounted in a 18.95-liter (5-gallon) covered stainless steel container or suspended straight in a polyethylene-lined trough.

In both configurations, the silicone tubing was completely immersed in deionized water saturated with excess solid ester. High agitation of the saturated reservoir solution outside the tubing was maintained in the stainless steel container by a 10-cm magnetic stirring bar rotated at 600 rpm and in the trough with three magnetic stirrers and two overhead stirrers placed along its length. High agitation was required to maintain saturation and to minimize transport resistance in the reservoir solution. Temperature was ambient (23–25°). Slight variations in temperature were compensated for by measuring the saturation concentration, C_s, at regular intervals during each study.

The silicone tubing, immersed in the saturated ester solution, was attached to either a two-stage syringe pump[4] or a reciprocating pump[5] with polyethylene and stainless steel tubing. The pump was connected to a supply of deionized water, which was pumped through the tubing at a

[1] Ethyl *p*-aminobenzoate from Eastman; butyl *p*-aminobenzoate from Matheson, Coleman and Bell.
[2] Silastic, Dow Corning, Midland, Mich.
[3] Beckman DB or Zeiss DMR21 recording spectrophotometer.
[4] Model 220, Sage Instruments, Cambridge, Mass.
[5] Single stream type B, Zenith Products, West Newton, Mass.

constant flow rate. Samples of the effluent solution were collected and assayed for the concentration, C_{av}, of ester at each flow rate.

RESULTS AND DISCUSSION

Figure 3 shows the results of transport studies carried out with the hexyl, butyl, and ethyl esters. It is quite apparent that the plug flow model (Eq. 2) is not applicable to any of the systems. This result was not unexpected, since plug flow is not applicable to Newtonian liquids under laminar flow conditions in a tube. The parabolic model (and its asymptotic solution at low Z) is apparently applicable to hexyl ester throughout the range of Z values studied, while butyl and ethyl esters exhibited varying degrees of negative deviations from the parabolic model.

For hexyl *p*-aminobenzoate (Fig. 3), the parabolic model fits the data well enough to confirm that the convective diffusional contribution to mass transfer can be predicted with a high degree of accuracy. All of the constants (D_{aq}, L, V_{av}, C_s, R, a_n, and b_n) found in Eq. 4 were independently obtained and used to calculate Z and the theoretical curve. Therefore, once C_{av} was determined at a particular V_{av}, no empirical fitting or correction was required to obtain the observed correlation between theory and experiment found in Fig. 3. One must be cautious, however, in interpreting these data with regard to the membrane transport of hexyl *p*-aminobenzoate through dimethyl polysiloxane, because, in fact, only the convective diffusional contribution to mass transfer was characterized.

Without the butyl and ethyl ester studies as a comparison, little can be said about the permeability characteristics of the hexyl ester through dimethyl polysiloxane, except that it is much higher than the convective diffusional resistance in the flowing liquid. Thus, the transport rate of a solute such as hexyl *p*-aminobenzoate in this tubular membrane system is completely governed by the bulk hydrodynamics of the system and not the membrane permeability. Such behavior is not unexpected, in general, and was demonstrated in similar transport systems (12). The value of these observations on hexyl *p*-aminobenzoate lies in the fact that the convective diffusional contribution can be calculated *a priori* with the aforementioned parameters and equations and compared with experimental results.

For a convective diffusion-controlled system, close control is required over the experimental conditions to obtain reproducible results. In the case of the hexyl ester (Fig. 3), when the circular tube configuration was employed, C_{av}/C_s values (open points) were consistently higher than predicted by theory, particularly at low Z (high flow rate). This positive deviation arose from secondary flows in the flowing liquid due to centrifugal forces which increase with flow rate (13). This effect essentially increases the convective contribution to mass transfer, allowing the liquid to take up more solute from the wall than would be predicted under purely laminar flow conditions. These secondary flows do not significantly affect the butyl and ethyl ester studies because both are in at least partial membrane control at Z values (<0.1) where the centrifugal effect becomes important. Twisting the tubing into irregular configurations induces turbulent flow conditions which gives rise to even greater positive deviations from theory than are observed with the circular configuration.

Butyl *p*-aminobenzoate (Fig. 3) exhibited the same adherence to the parabolic model as the hexyl ester at large Z (low flow rates) but deviated negatively at small Z (high flow rates). Such behavior indicates that, at low flow rates, butyl *p*-aminobenzoate transport is purely convective diffusion controlled but that membrane transport resistance becomes limiting at high flow rates. As can be seen from Fig. 3 at the lowest Z values studied, the log–log plot of C_{av}/C_s *versus* Z is linear with a slope of approximately 1, indicating that the system is completely membrane controlled. This graphical characteristic allows the differentiation of complete convective diffusion control and membrane control in a laminar flow tubular membrane system; the former exhibits a slope of two-thirds for a log–log plot of C_{av}/C_s *versus* Z, while the latter gives a slope of 1.

The transition region over which the type of transport control changes depends upon the solute, membrane properties, and hydrodynamic conditions. Comparison of the butyl and hexyl esters shows that the important physicochemical difference lies in their membrane–water partition coefficients, P. There is approximately a 10-fold difference in the partition coefficients of the butyl and hexyl esters (Table I), which would predict an order of magnitude lower membrane permeability for butyl *p*-aminobenzoate compared to hexyl *p*-aminobenzoate. With lower membrane permeability, the butyl ester begins to show membrane control at $C_{av}/C_s \simeq 0.1$; it can be estimated that the hexyl ester would begin to exhibit membrane control at $C_{av} \simeq 0.01$, which is above the range of flow rates used.

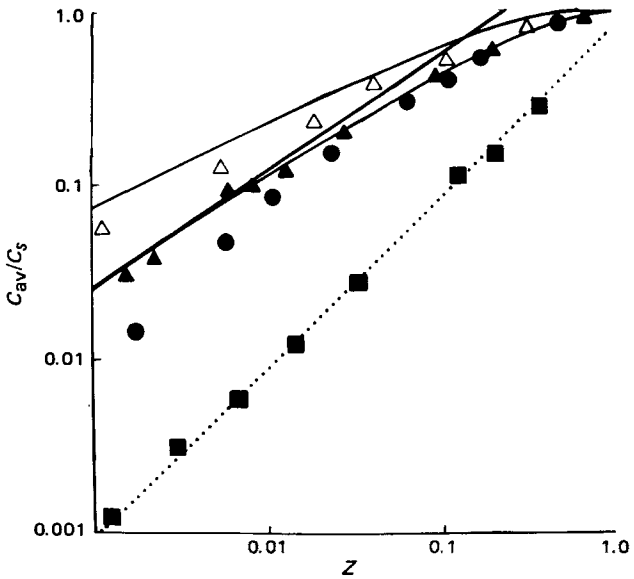

Figure 3—*Log–log plot of* C_{av}/C_s versus Z *for* p-*aminobenzoate esters. Key:* ▲, *hexyl ester (straight tube configuration);* △, *hexyl ester (curved tube configuration);* ●, *butyl ester;* ■, *ethyl ester;* —, *theoretical predictions as labeled in Fig. 2; and . . ., plot of Eq. 9 for the ethyl ester.*

By comparing the data obtained for butyl *p*-aminobenzoate to the predictions in Fig. 2, a value for R_w of 0.1–0.2 can be estimated. With values of D_m, D_{aq}, and P in Table I and the tubing dimensions, R_w was determined to be 0.15 using Eq. 7. Such a correlation between experiment and theory under membrane-controlled conditions further supports the utility of tubular membrane systems for determining the relative importance of membrane permeability and convective diffusion to overall transport rates.

The results for ethyl *p*-aminobenzoate (Fig. 3), in contrast to the previous two esters, fall significantly below theoretical convective diffusion predictions. Throughout the range of flow rates studied, the ethyl ester remained in essentially complete membrane control. Studies at very low flow rates (not shown) indicate that ethyl *p*-aminobenzoate approaches $C_{av}/C_s = 1$ at $Z > 1$. Using values for D_m, D_{aq}, and P found in Table I for the ethyl ester with Eq. 7 leads to a predicted R_w of 2.08, which indicates that membrane resistance is high and that convective diffusion is unimportant to mass transfer over the range of flow rates studied. As with the butyl ester at low Z, the log–log plot of C_{av}/C_s *versus* Z for the ethyl ester exhibits a slope of 1, indicating that the solute flux through the membrane is constant and maximal and that changes in C_{av}/C_s with Z only reflect a change in throughput of liquid.

Under complete membrane control, the transport rate is independent of hydrodynamics (laminar or turbulent flow). As a test of this independence, Eq. 8 (14), which predicts the flux, F, through a cylindrical wall at steady state with the inner wall at zero concentration and the outer wall in contact with a saturated solution, was employed:

$$F = \frac{2\pi D_m P C_s}{\ln (\text{o.d./i.d.})} \qquad \text{(Eq. 8)}$$

Since F is the flux per unit length, multiplying by the tube length, L, dividing by the volume flow rate, f, and rearranging give:

$$\frac{C_{av}}{C_s} = \frac{2\pi D_m P L}{f \ln(\text{o.d./i.d.})} \qquad \text{(Eq. 9)}$$

Using the parameters from Table I and the tubing dimensions gives $C_{av}/C_s = 0.116/f$, which is plotted in Fig. 3 (dotted line). Such a close correlation between the experimental C_{av}/C_s values and Eq. 9 confirms the independence of ethyl *p*-aminobenzoate transport from hydrodynamics, since no account is taken of the type of convection in obtaining Eq. 9. Thus, the flowing fluid serves only to carry the ethyl ester from the inner tubing wall and provides no detectable resistance to solute transport.

With the three *p*-aminobenzoate esters chosen for study, three typical transport patterns were demonstrated: the extremes of complete membrane (ethyl ester) and complete convective diffusion (hexyl ester) control and a change in transport control with flow rate (butyl ester). The ability to calculate accurately, *a priori*, the influence of hydrodynamics is unattainable by other experimental designs. These studies, of course, do not detract from previous membrane transport work in which stagnant

liquid diffusion layers were employed in the theoretical analysis (1, 3). Rather, this work demonstrates that such diffusion layers are in reality convenient "fictions," which need not be invoked with certain experimental designs. Certainly, the concept of aqueous diffusion layers has been instrumental in the understanding of membrane transport processes, but too much credence has been given to their actual existence.

Biological analogies to these polymeric tube transport studies are the isolated perfusion and *in situ* techniques for intestinal absorption. An isolated intestinal segment suspended as nearly straight as possible would serve as a means for determining the luminal convective diffusion contribution to intestinal transport. For an *in situ* intestinal system, definite bends in the intestine would induce secondary flows or turbulence, which would require that absorption data be carefully analyzed for the demarcation between convective diffusion control and membrane control. With the ability to determine accurately the luminal contribution to overall intestinal transport, absorption models can be established on a firmer physical basis. Without the need for semiempirical approaches to obtain diffusion layer or stagnant film permeability coefficients, the elucidation of membrane transport characteristics should be facilitated.

Furthermore, the tube configuration is of value pharmaceutically for obtaining the intrinsic dissolution rates of solids (9). Solid tubes, obtained by various methods, can be infused with dissolution media and the efflux concentrations can be measured as a function of flow rate. From such information, the presence or absence of surface or other kinetic barriers can be determined by comparison of efflux concentrations with the theoretical predictions for pure convective diffusion control.

REFERENCES

(1) R. G. Stehle and W. I. Higuchi, *J. Pharm. Sci.*, **61**, 1922, 1931 (1972).

(2) E. R. Garrett and P. B. Chemburkar, *ibid.*, **57**, 944, 949; 1401 (1968).

(3) G. L. Flynn and S. H. Yalkowsky, *ibid.*, **61**, 838 (1972).

(4) N. Lakshminarayanaiah, "Transport Phenomena in Membranes," Academic, New York, N.Y., 1969.

(5) V. G. Levich, "Physicochemical Hydrodynamics," Prentice-Hall, Englewood Cliffs, N.J., 1962, pp. 40–46.

(6) J. G. Knudsen and D. L. Katz, "Fluid Dynamics and Heat Transfer," McGraw-Hill, New York, N.Y., 1958, pp. 82–87.

(7) G. M. Brown, *A.I.Ch.E.J.*, **6**, 179 (1960).

(8) V. G. Levich, "Physicochemical Hydrodynamics," Prentice-Hall, Englewood Cliffs, N.J., 1962, p. 115.

(9) W. H. Linton and T. K. Sherwood, *Chem. Eng. Progr.*, **46**, 258 (1950).

(10) J. Schenk and J. M. Dumoré, *Appl. Sci. Res.*, **A4**, 39 (1954).

(11) R. G. Buckles, E. W. Merrill, and E. R. Gilliland, *A.I.Ch.E.J.*, **14**, 703 (1968).

(12) R. E. Collingham, P. L. Blackshear, and E. R. G. Eckert, *Chem. Eng. Progr. Symp. Ser. 102*, **66**, 141 (1970).

(13) Y. Mori and W. Nakayama, *Int. J. Heat Mass Transfer*, **10**, 681 (1967).

(14) M. H. Jacobs, "Diffusion Processes," Springer-Verlag, New York, N.Y., 1967, p. 120.

(15) G. L. Flynn, S. H. Yalkowsky, and T. J. Roseman, *J. Pharm. Sci.*, **63**, 479 (1974).

ACKNOWLEDGMENTS AND ADDRESSES

Received February 9, 1976, from the *School of Pharmacy, University of Connecticut, Storrs, CT 06268, and the ‡Pharmacy Research Unit, The Upjohn Company, Kalamazoo, MI 49001.

Accepted for publication May 5, 1976.

Support for this study in the form of a Summer Visiting Professorship from The Upjohn Co. is gratefully acknowledged by D. R. Flanagan.

ˣ To whom inquiries should be directed.

Quantitative Determination of Phenacetin and Its Metabolite Acetaminophen by GLC–Chemical Ionization Mass Spectrometry

W. A. GARLAND *ˣ, K. C. HSIAO ‡, E. J. PANTUCK ‡, and A. H. CONNEY *

Abstract □ A quantitative GLC–mass spectrometric procedure was developed for the determination of phenacetin and its *O*-desethyl metabolite, acetaminophen, in human plasma. The assay utilizes selective ion detection to monitor, in a GLC effluent, the MH^+ molecular ions of both phenacetin and the methyl derivative of acetaminophen, *p*-acetanisidine, generated by isobutane chemical ionization. Deuterated analogs of phenacetin and acetaminophen, phenacetin-d_3 and acetaminophen-d_3, respectively, are added to the plasma before extraction to serve as internal standards. To determine phenacetin and unconjugated acetaminophen, 1.0 ml of plasma is extracted with 5 ml of benzene–dichloroethane (7:3). The extraction solvent is removed, and the residue is methylated with diazomethane. The solution is again evaporated to dryness, and the residue is reconstituted in ethyl acetate. A portion of this solution is then analyzed by GLC–mass spectrometry, with the mass spectrometer set to monitor *m/e* 166 (*p*-acetanisidine), 169 (*p*-acetanisidine-d_3), 180 (phenacetin), and 183 (phenacetin-d_3). To determine total acetaminophen, 0.1 ml of plasma is treated with a mixture of β-glucuronidase and sulfatase, extracted with ethyl acetate, methylated, and analyzed by GLC–mass spectrometry. The procedure has a sensitivity limit of 1 ng of phenacetin/ml and 0.1 μg of acetaminophen/ml. The curves relating the amount of phenacetin and acetaminophen added *versus* the amount of phenacetin and acetaminophen found for 12 known phenacetin concentrations over the 9.9–246.6-ng/ml range and for 16 known acetaminophen concentrations over the 0.52–13.10-μg/ml range are straight lines with intercepts of nearly zero and with slopes of unity. Analyses of six separate plasma samples, each containing 25 ng of phenacetin/ml and 1.31 μg of acetaminophen/ml, had a precision of ±1 ng/ml for phenacetin and ±0.08 μg/ml for acetaminophen.

Keyphrases □ Phenacetin—GLC–mass spectrometric analysis, human plasma □ Acetaminophen—GLC–mass spectrometric analysis, human plasma □ GLC–mass spectrometry—analyses, phenacetin and acetaminophen, human plasma □ Analgesics—phenacetin and acetaminophen, GLC–mass spectrometric analysis, human plasma

Various nonspecific spectrophotometric (1–5) procedures or time-consuming liquid (6, 7), paper (8, 9), or thin-layer (10–12) chromatographic procedures have been developed to measure the analgesic phenacetin (I) and its analgesic biotransformation product, acetaminophen (II), in human plasma. The published GLC procedures for these compounds have a detection limit of 50 ng/ml (13–15). While this sensitivity is suitable for the measurement of